

Lattice calculation of Collins-Soper Kernel

Hai-Tao Shu¹

¹ University of Regensburg - Institute for Theoretical Physics

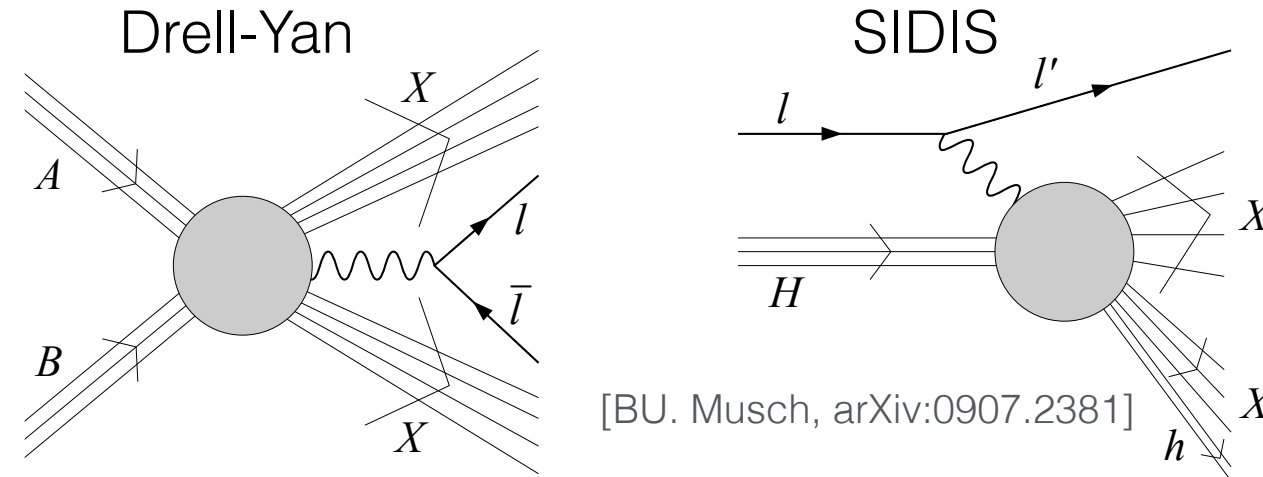


arXiv: 2302.06502
arXiv: 2302.xxxxx

FOR 2926
Feb. 16-17, 2023, Regensburg

From TMDs to Collins-Soper kernel

- TMDs universal in Drell-Yan process and semi-inclusive deep inelastic scattering



- CS kernel encodes the rapidity scaling properties of transverse momentum dependent parton distribution functions (TMDPDFs) / wave functions (TMDWFs):

$$2\zeta \frac{d}{d\zeta} \ln f^{\text{TMD}}(x, b_\perp, \mu, \zeta) = K(b_\perp, \mu)$$

- Extraction of CS kernel on the lattice:

- From ratio of TMDWFs within LaMET [M. A. Ebert, L. W. Stewart and Y. Zhao, PRD 99, 034505]
- From ratio of TMDPDFs using Mellin moments [A. A. Vladimirov and A. Schaefer, PRD 101, 074517]
- An application of CS kernel: from quasi TMDs to physical TMDs [X. Ji and Y. Liu, PRD105,076014]

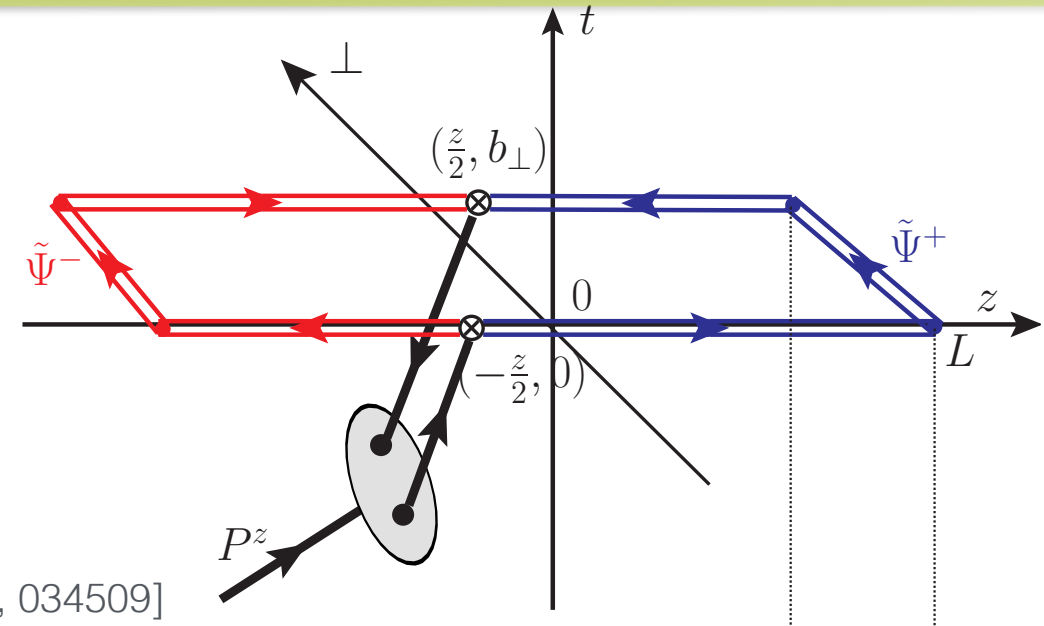
$$\tilde{\Psi}^+(x, b_\perp, \mu, \zeta_z) S_r^{1/2}(b_\perp, \mu) = H^+(\zeta_z, \bar{\zeta}_z, \mu^2) \exp \left[\frac{1}{2} K(b_\perp, \mu) \ln \frac{-\zeta_z - i\epsilon}{\zeta} \right] \Psi^+(x, b_\perp, \mu, \zeta) + \mathcal{O}\left(\frac{\Lambda_{QCD}^2}{\zeta_z}, \dots\right)$$

Determine CS kernel within LaMET

- Factorization based on LaMET using TMDWFs:

$$K(b_\perp, \mu, x, P_1^z, P_2^z) = \frac{1}{\ln(P_1^z/P_2^z)} \ln \frac{H^-(xP_2^z, \mu)\Psi(x, b_\perp, \mu, P_1^z)}{H^-(xP_1^z, \mu)\Psi(x, b_\perp, \mu, P_2^z)}$$

- Leading order matching: [Q.A. Zhang et al., PRL125, 192001]
[Yuan Li et al, PRL.128(2022)6,062002]
- Next-to-leading order matching: [M.-H. Chu et al, PRD 106 (2022) 3, 034509]



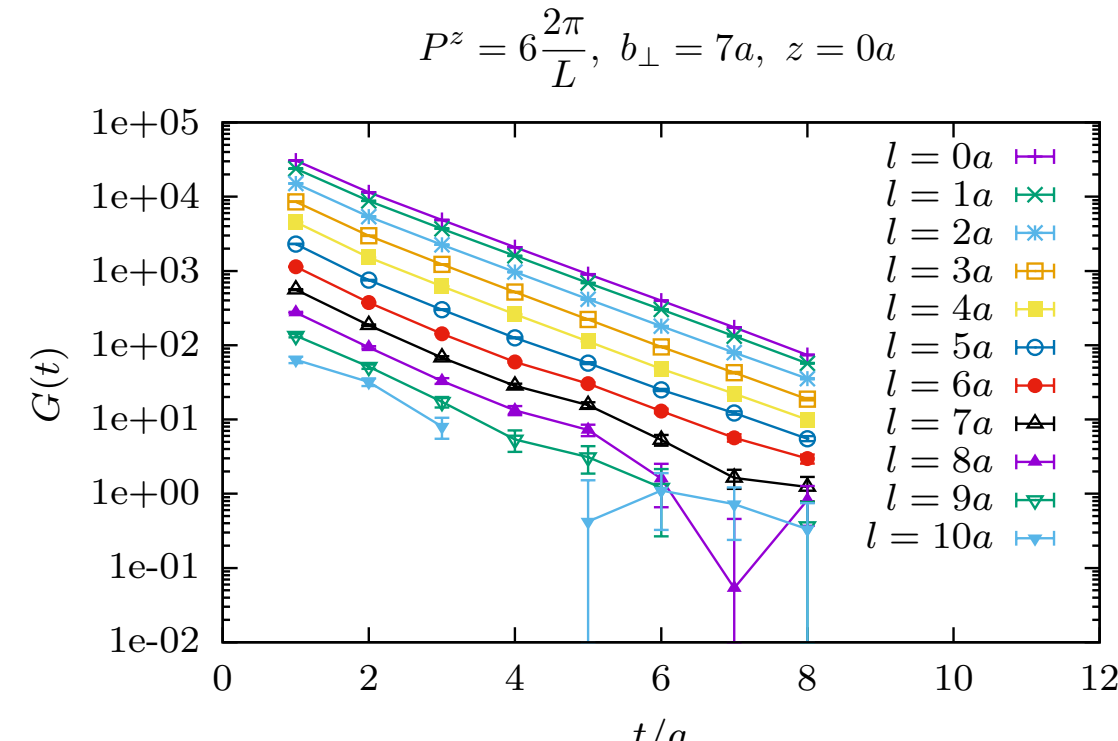
Goal of this study → A NLO CS kernel for CLS ensemble

- Quasi TMD wave functions:

$$\phi_l(z, b_\perp, P^z, l) = \langle 0 | \bar{\psi}(\vec{z}/2 + \vec{b}) \Gamma \mathcal{W}(\vec{b}, l) \psi(-\vec{z}/2) | \pi(\vec{P}) \rangle$$

- Quasi TMD wave functions from 2pt functions:

$$\begin{aligned} C_{\Gamma_\phi}^{2pt}(b_\perp, l, P^z, t) &= \frac{Z_\phi}{L^3} \sum_{\vec{x}} e^{-iP^z x_z} \langle O_\phi(t, b_\perp, l) O_\pi^\dagger(0, P^z) \rangle \\ &= \frac{A_w(p_z) A_p}{2E} e^{-Et} \phi_\ell(0, b_\perp, P^z, \ell) (1 + c_0 e^{-\Delta E t}) \end{aligned}$$



Joint fit of all l&b (sharing energies) for each P^z

Lattice setup

- We use newly generated 2+1 flavor clover fermion CLS ensemble X650

β	$L^3 \times T$	a	m_π^{sea}	m_π^v	#conf
3.34	$48^3 \times 48$	0.098 fm	333 MeV	662 MeV	1000

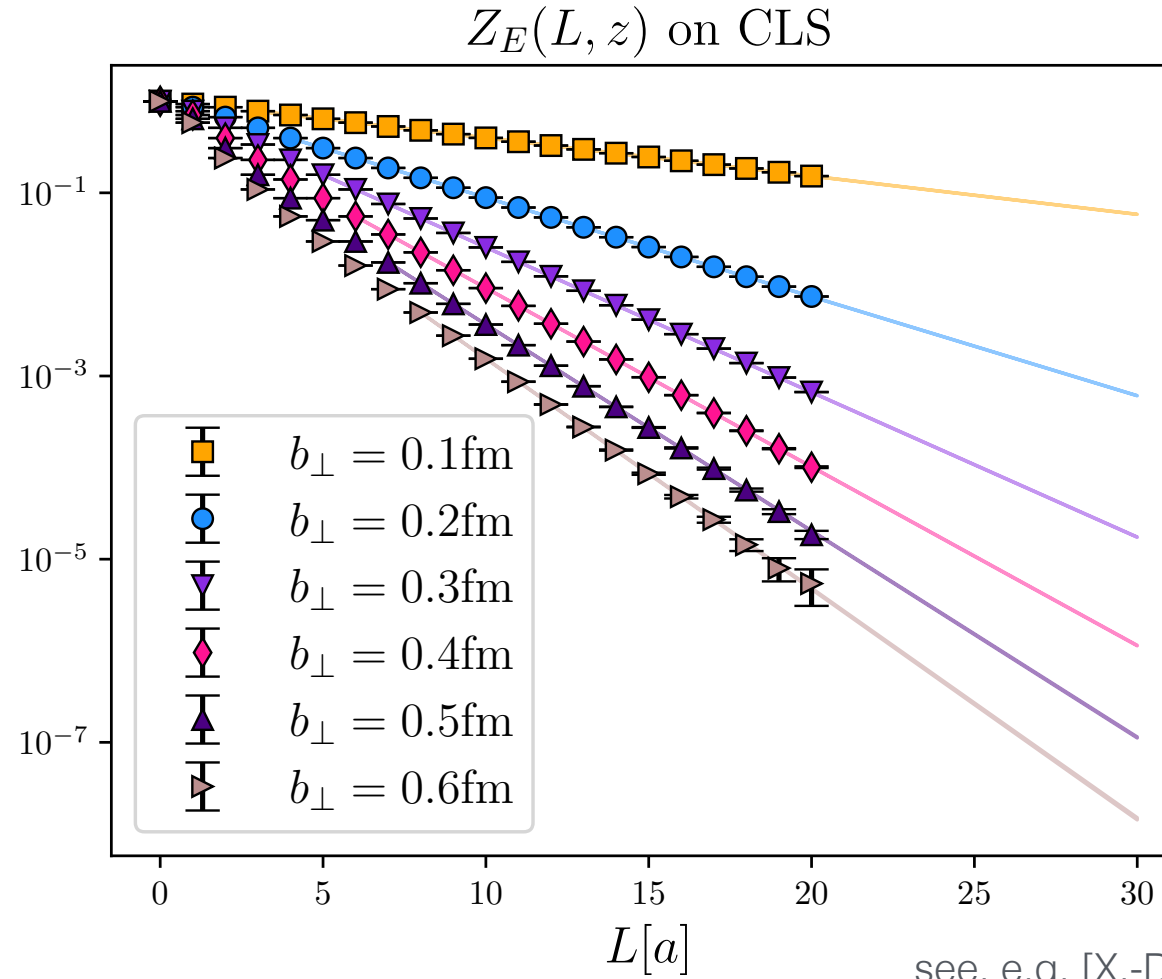
- HYP smearing + Wall source
- 2 sources per configuration
- Transverse direction: x and y
- Momenta: $P_z = \{0, 6, 8, 10, 12\} \times 2\pi/L$
(i.e. 0, 1.6, 2.1, 2.6, 3.2 GeV)
- $0 \leq l/a \leq 10, 0 \leq b/a \leq 7, 0 \leq t/a \leq 9$

Renormalization of the quasi TMDWFs (I)

[LPC, PRL 129 (2022) 082002]

$$\tilde{\Psi}^\pm(x, b_\perp, \mu, \zeta^z) = \lim_{L \rightarrow \infty} \int \frac{P^z dz}{2\pi} e^{ixzP^z} \frac{\tilde{\Psi}^\pm(z, b_\perp, \mu, P^z)}{\sqrt{Z_E(2L \pm z, b_\perp, \mu)} Z_O(1/a, \mu, \Gamma)}$$

- The linear divergence and heavy quark potential is removed by Wilson loop Z_E
- Residual logarithmic divergence is removed by Z_O



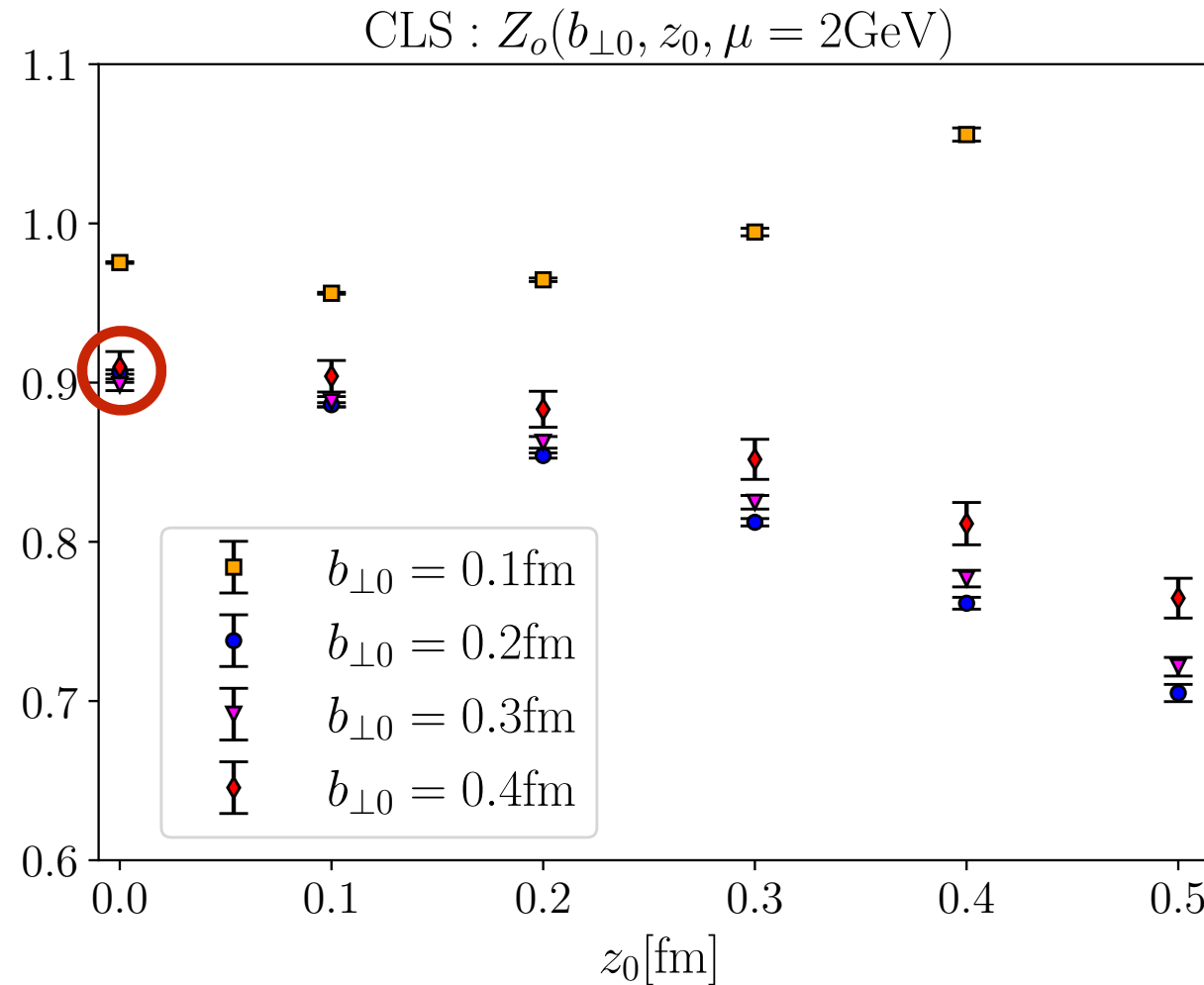
- Large L limit not available on the lattice
- Extrapolation to large L with 1-state fit

Renormalization of the quasi TMDWFs (II)

$$\tilde{\Psi}^\pm(x, b_\perp, \mu, \zeta^z) = \lim_{L \rightarrow \infty} \int \frac{P^z dz}{2\pi} e^{ixzP^z} \frac{\tilde{\Psi}^\pm(z, b_\perp, \mu, P^z)}{\sqrt{Z_E(2L \pm z, b_\perp, \mu)} Z_O(1/a, \mu, \Gamma)}$$

[LPC, PRL 129 (2022) 082002]

- The linear divergence and heavy quark potential is removed by Wilson loop Z_E
- Residual logarithmic divergence is removed by Z_O [LPC, PRL 129 (2022) 082002]



$$Z_O(1/a, \mu) = \frac{\tilde{\Psi}^{\pm,0}(z_0, b_{\perp 0}, \zeta^z = 0, L)}{\sqrt{Z_E(2L \pm z_0, b_{\perp 0}, \mu)} \tilde{\psi}^{\overline{\text{MS}}}(b_{\perp 0}, z_0, \mu)}$$

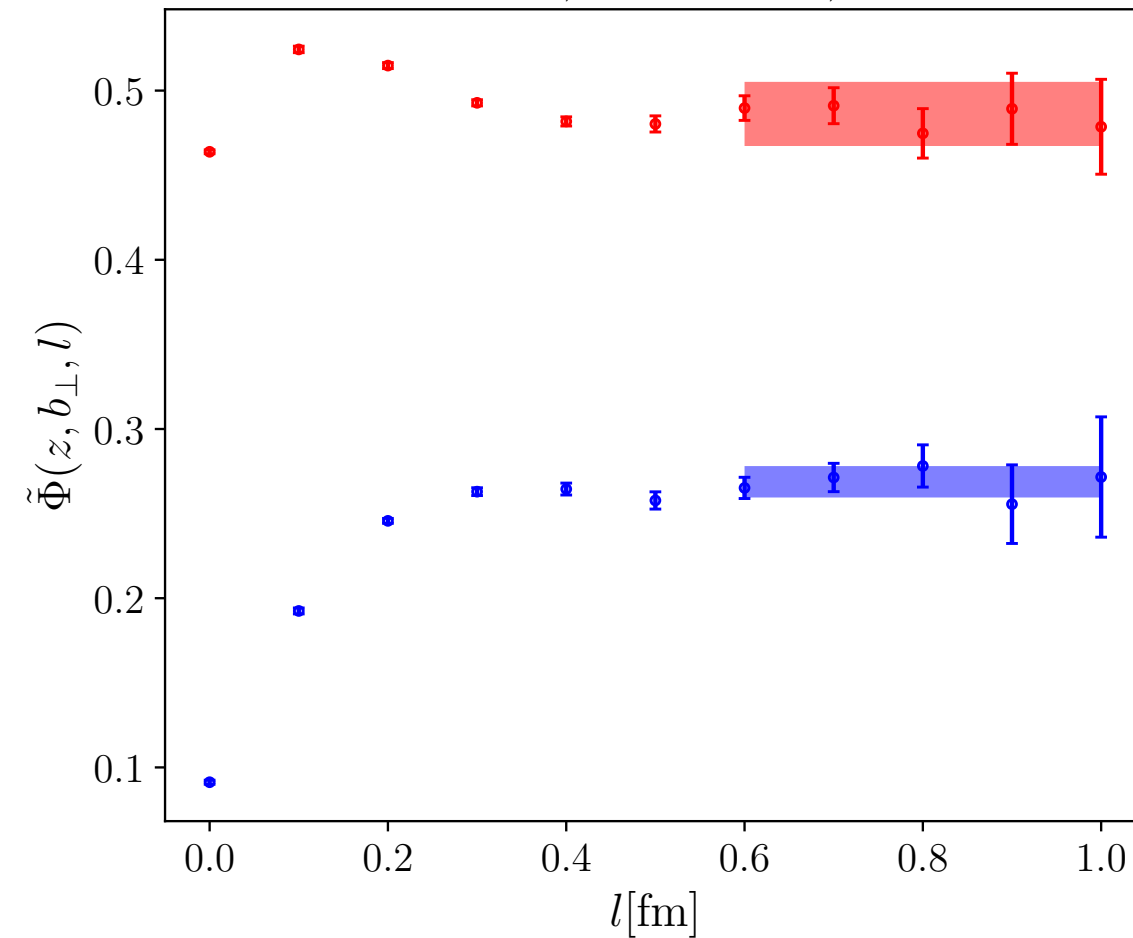
$$\tilde{\psi}^{\overline{\text{MS}}}(b_{\perp 0}, z_0, \mu) = 1 + \frac{\alpha_s C_F}{2\pi} \left\{ \frac{1}{2} + 3\gamma_E - 3\ln 2 \right.$$

$$\left. + \frac{3}{2} \ln[\mu^2(b_{\perp 0}^2 + z_0^2)] - 2 \frac{z_0}{b_{\perp 0}} \arctan \frac{z_0}{b_{\perp 0}} \right\} + \mathcal{O}(\alpha_s^2)$$

- Look for plateau in b where both discretization effects and higher twist contaminations are suppressed

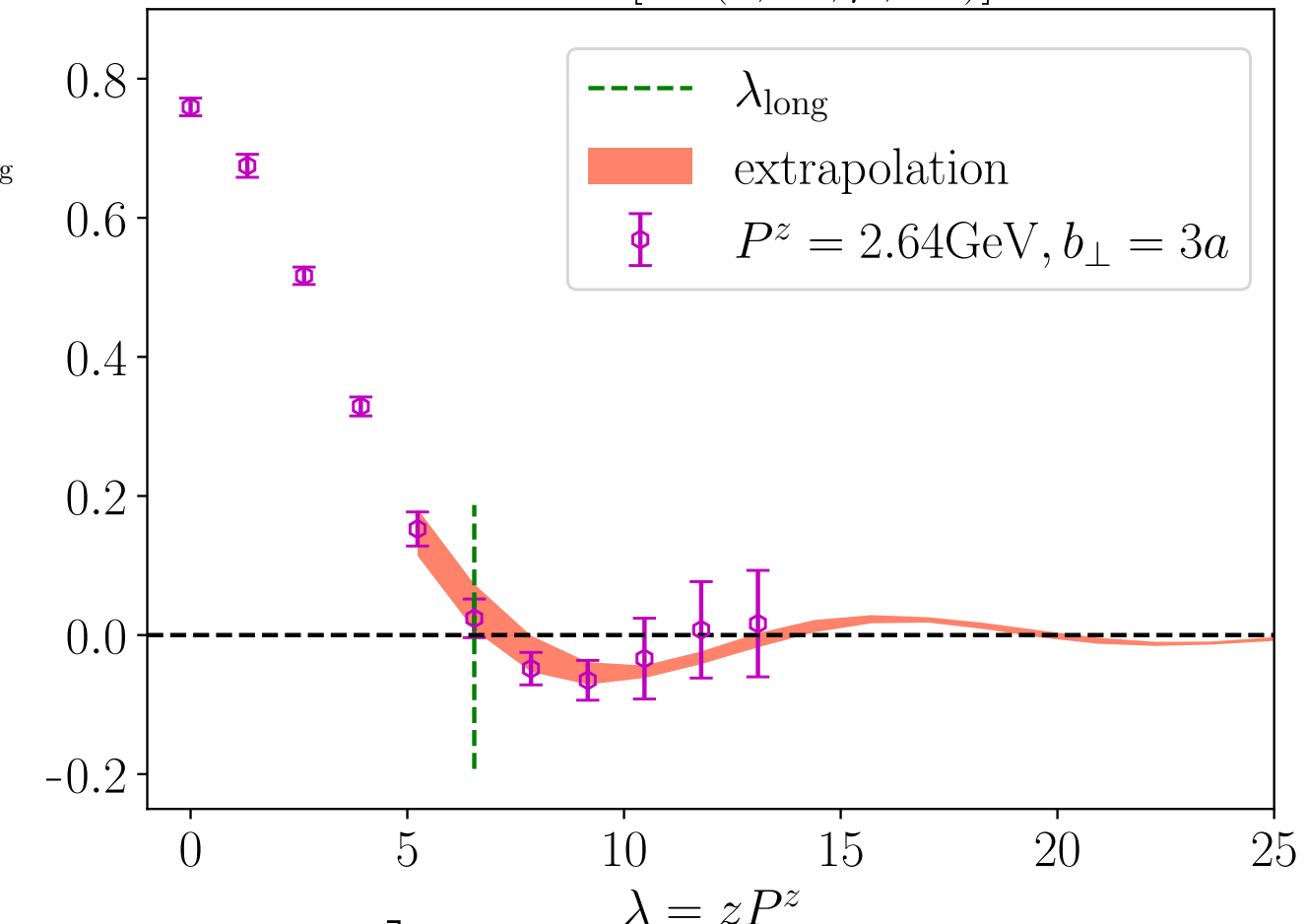
From position space to momentum space

$$P^z = 2.64 \text{ GeV}, b_\perp = 0.4 \text{ fm}, z = 0.2 \text{ fm}$$



fit, real
fit, imag
data, real
data, imag

$$\text{CLS : } \text{Re}[\tilde{\Psi}^-(z, b_\perp, \mu, P^z)]$$



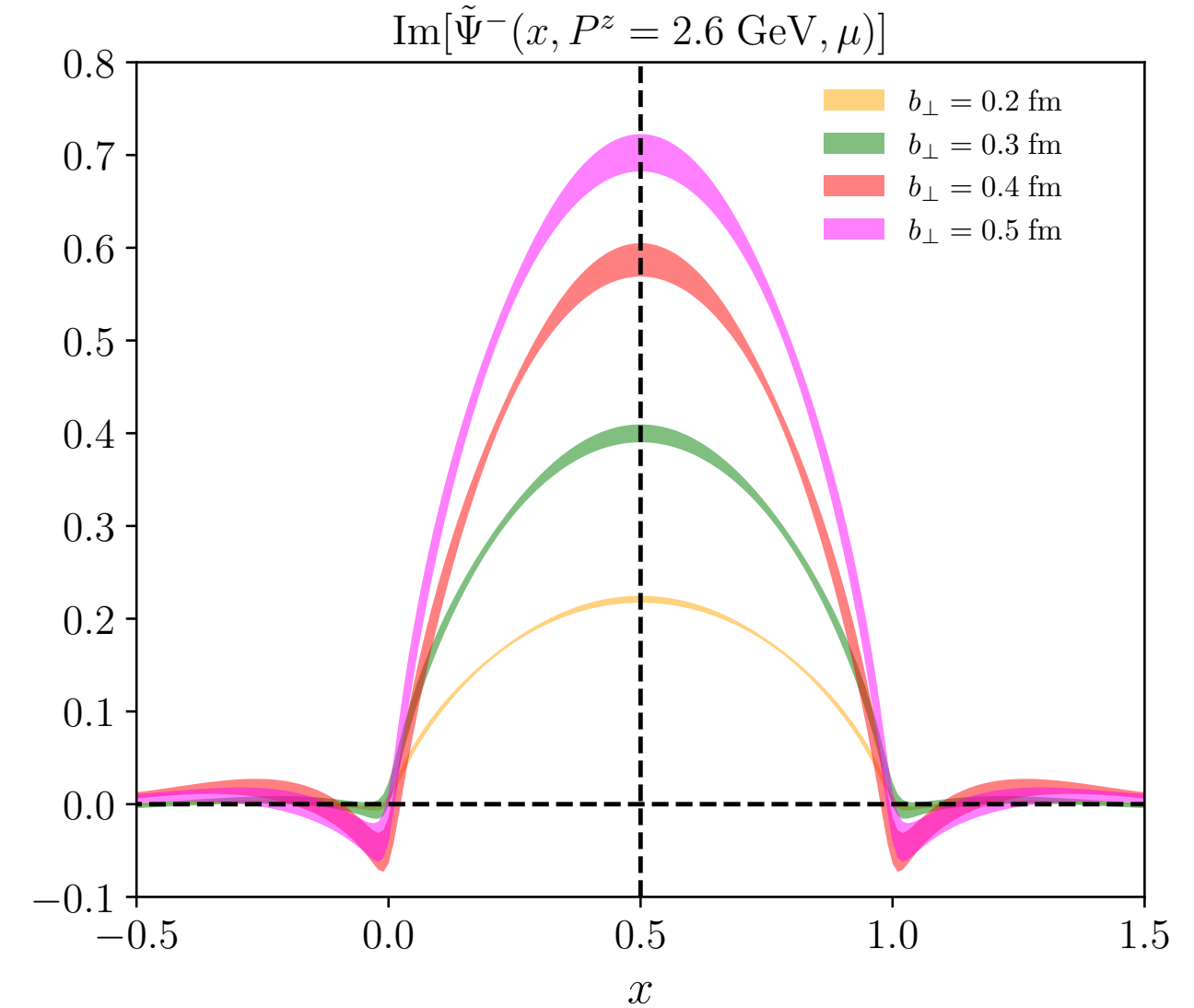
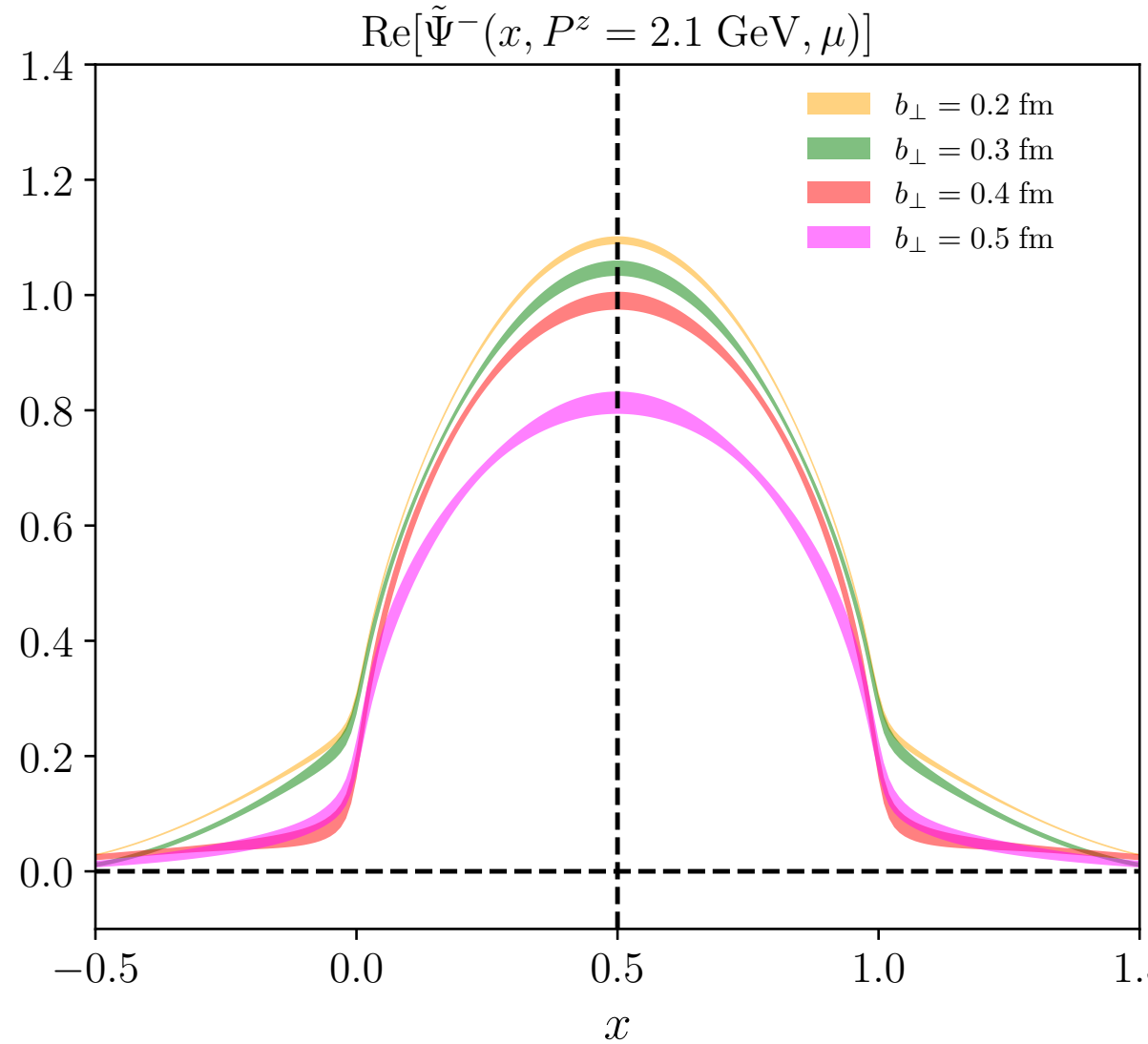
λ_{long}
extrapolation
 $P^z = 2.64 \text{ GeV}, b_\perp = 3a$

$$\tilde{\Psi}(z, b_\perp, \mu, \zeta^z) = f(b_\perp) \left[\frac{k_1}{(-i\lambda)^d} + e^{i\lambda} \frac{k_2}{(i\lambda)^d} \right] e^{-\frac{\lambda}{\lambda_0}}$$

- Large L limit via constant fit in plateau range ($L > \sim 0.7$ fm)
- Extrapolation for large lambda range using theoretically-inspired Ansatz [X.-D. Ji, et al., NPB 964 (2021) 115311]
- Fourier transformation going to momentum space

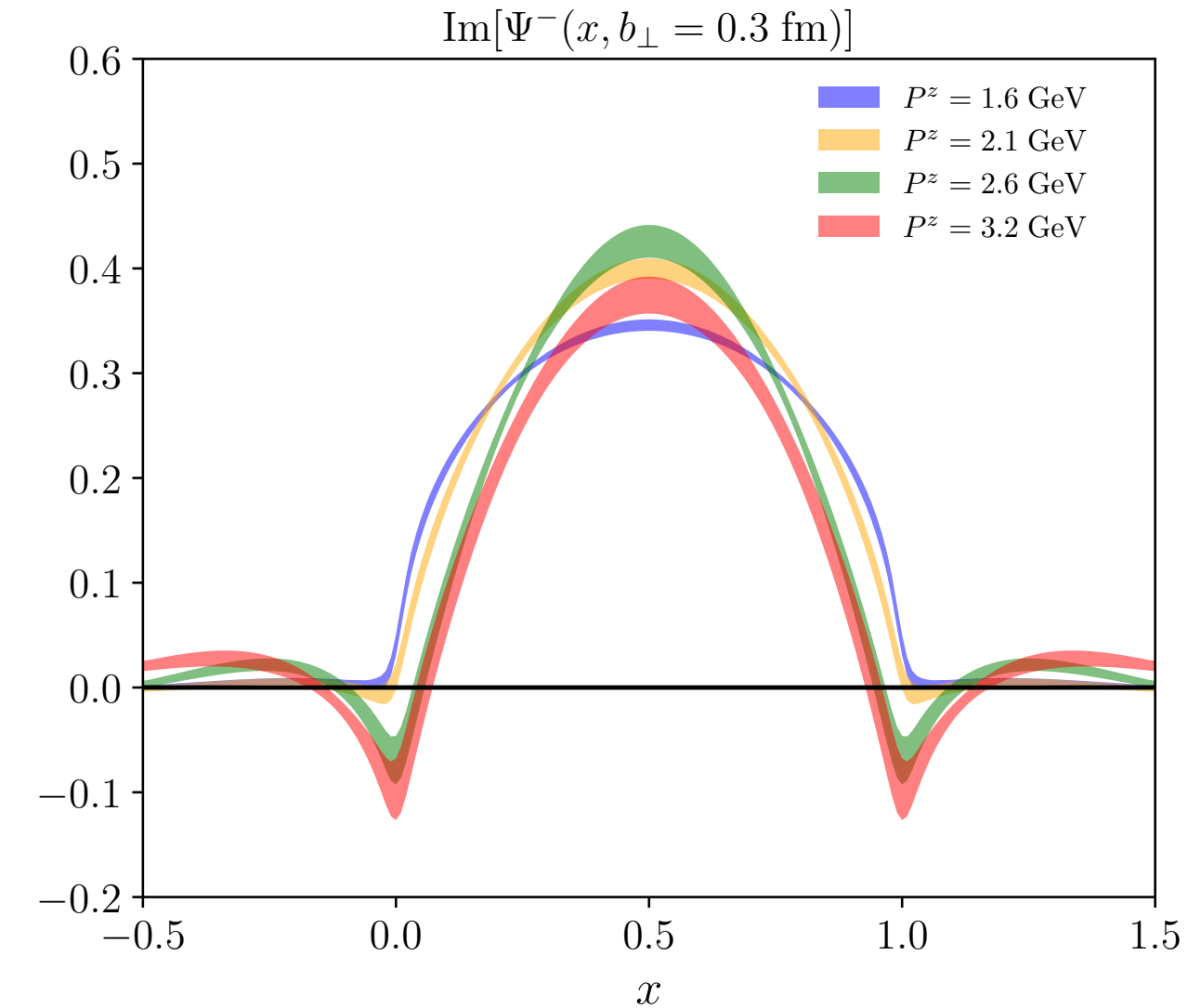
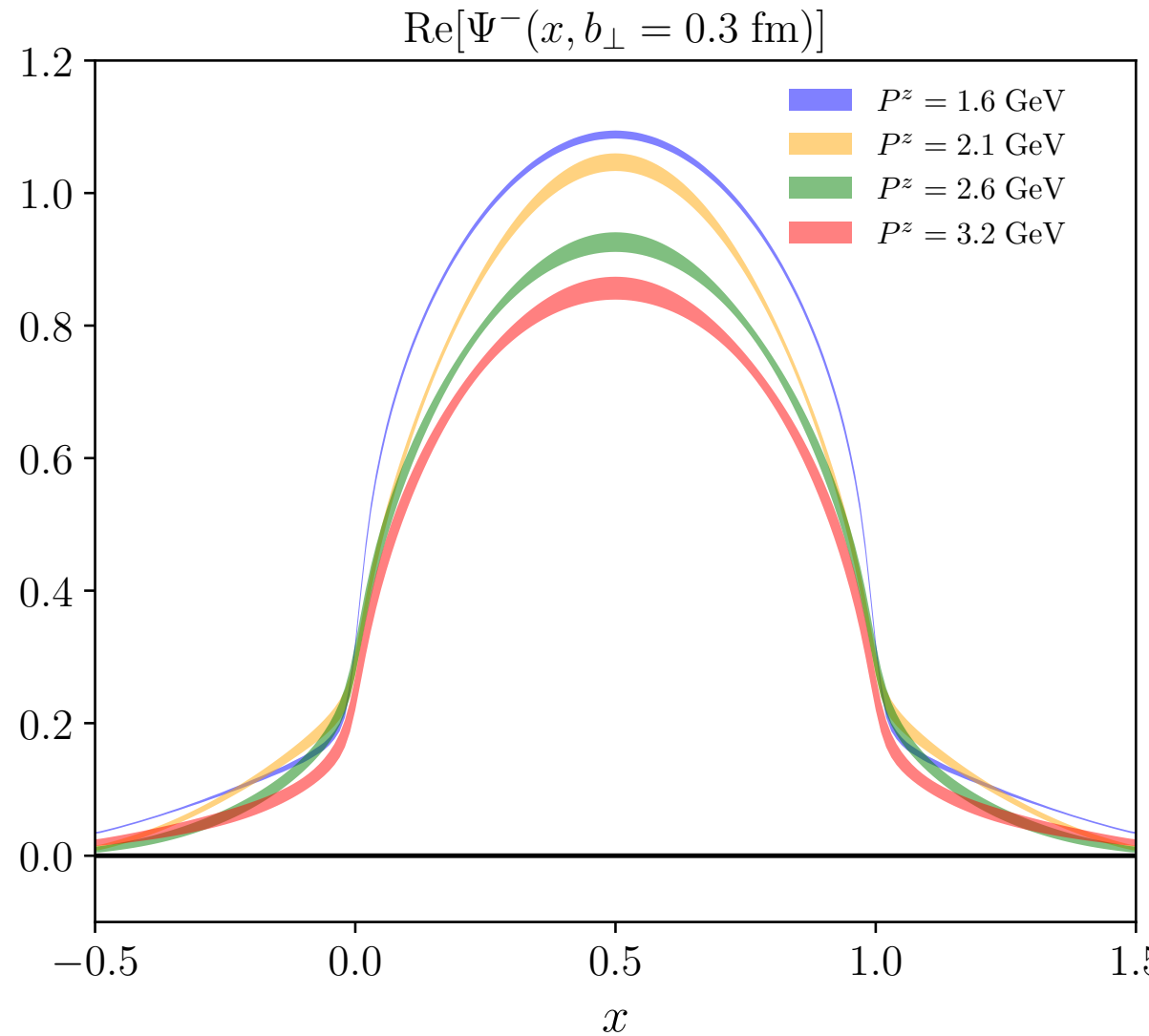
$$\tilde{\Psi}^\pm(x, b_\perp, \mu, \zeta^z) = \lim_{L \rightarrow \infty} \int \frac{P^z dz}{2\pi} e^{ixzP^z} \dots$$

Quasi TMDWFs in momentum space (I)



- Real part has larger amplitude at same b
- Clear dependence on b for both real and imaginary parts
- Stronger dependence on b for imaginary part

Quasi TMDWFs in momentum space (II)



- Real part has larger amplitude at same momentum
- Clear dependence on momentum for both real and imaginary parts
- Stronger dependence on momentum for real part

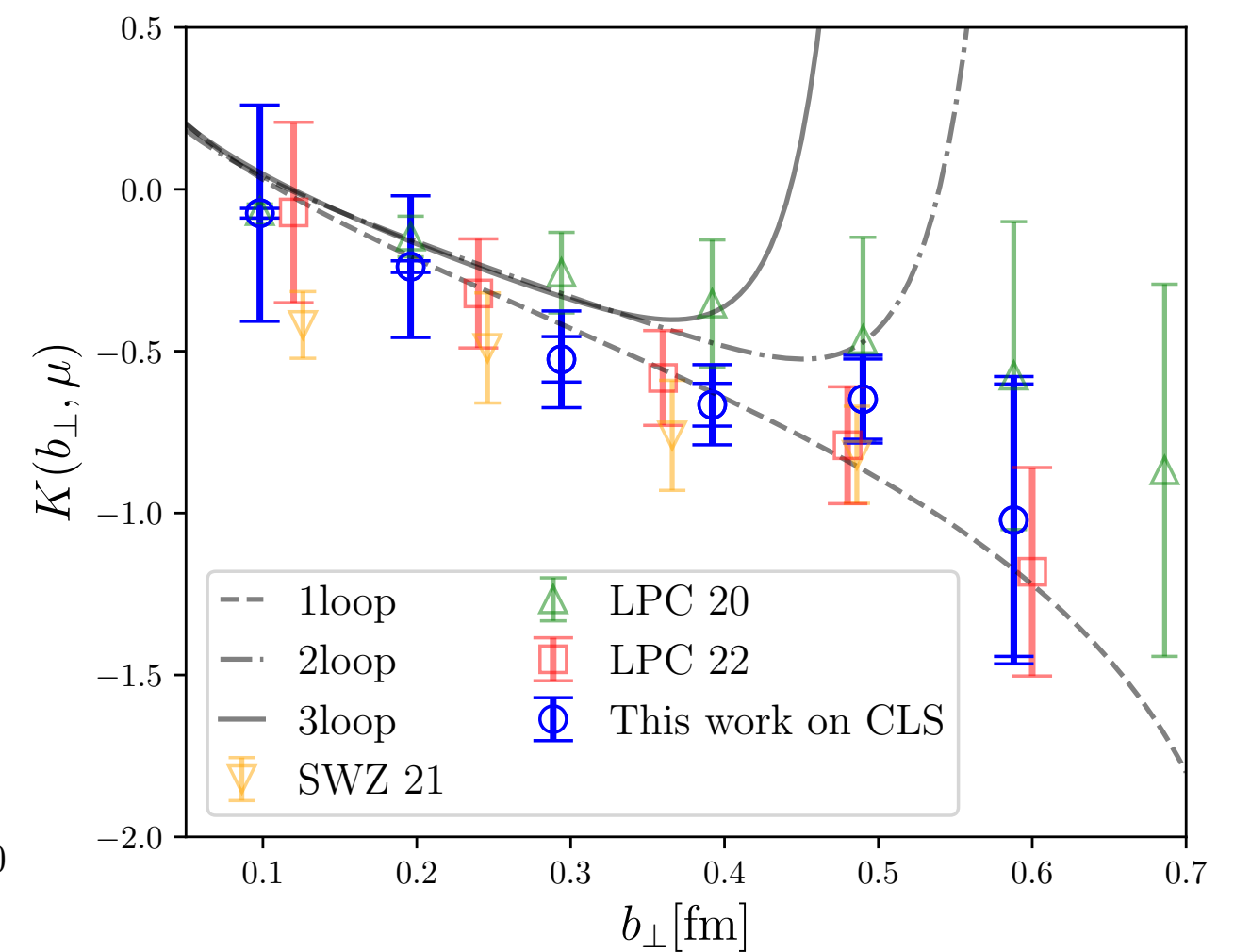
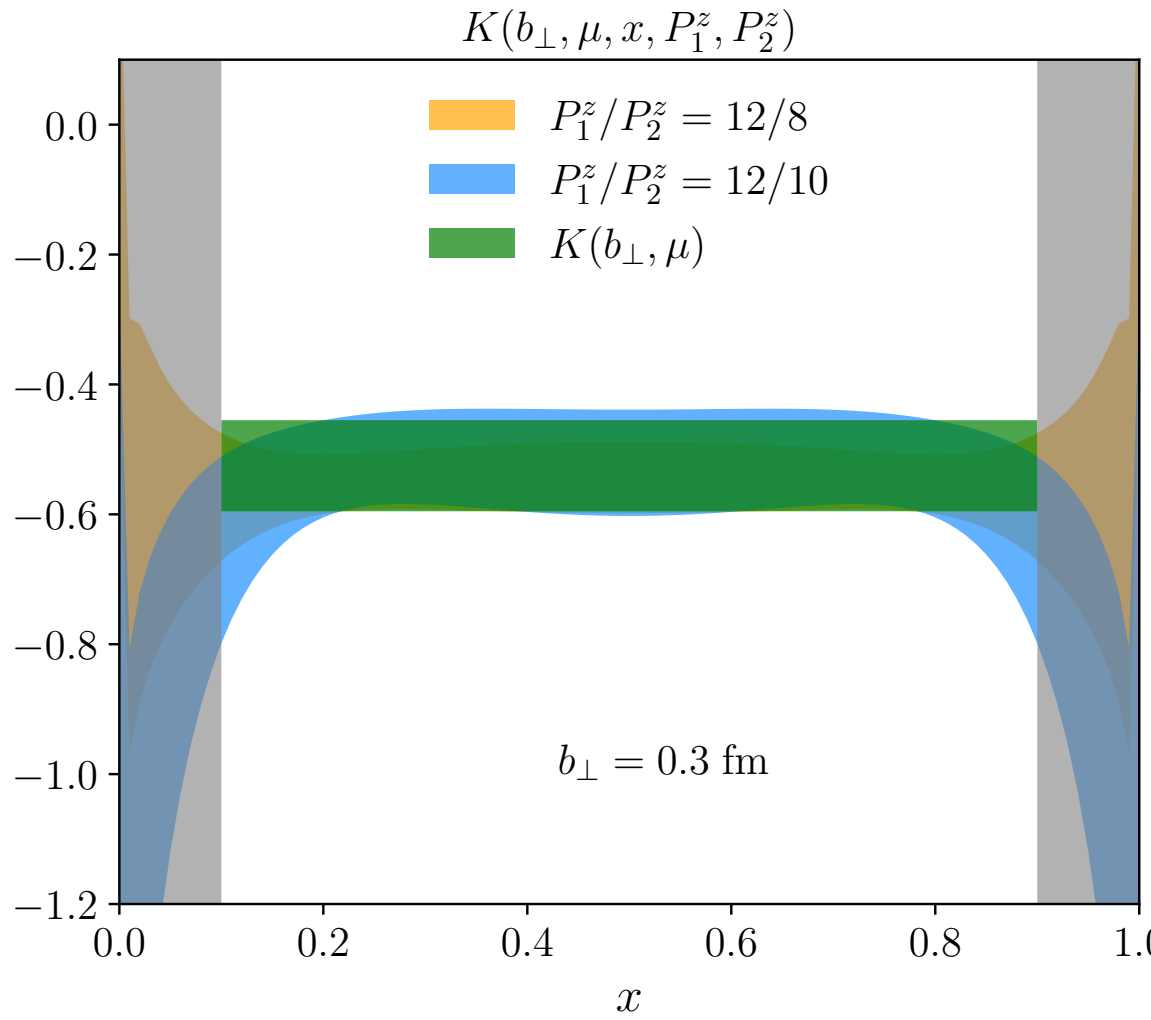
Collins-Soper kernel from LaMET

- 1-loop matching kernel H from: [X.-D. Ji and Y.-Z. Liu, PRD105, 076014]

$$K(b_\perp, \mu, x, P_1^z, P_2^z) = \frac{1}{\ln(P_1^z/P_2^z)} \ln \frac{H^-(xP_2^z, \mu)\Psi(x, b_\perp, \mu, P_1^z)}{H^-(xP_1^z, \mu)\Psi(x, b_\perp, \mu, P_2^z)}$$

- Extract leading power contribution via joint fit: [M.-H. Chu et al, PRD 106 (2022) 3, 034509]

$$K(b_\perp, \mu, x, P_1^z, P_2^z) = K(b_\perp, \mu) + A \left[\frac{1}{x^2(1-x)^2(P_1^z)^2} - \frac{1}{x^2(1-x)^2(P_2^z)^2} \right]$$



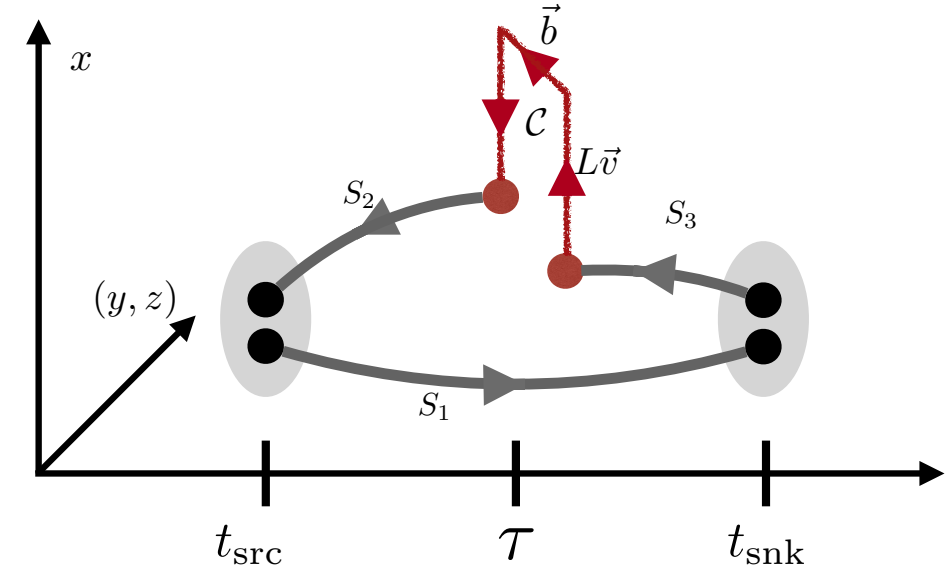
- Good agreement with previous lattice calculations

CS kernel from Mellin moments

- CS kernel from (first) Mellin moments of ratio of TMDPDFs:

$$\begin{aligned} R^{[\Gamma]}(x, b, \mu; P_1, P_2) &= \frac{W_{f/h}^{[\Gamma]}(x, b; P_1, S; \mu)}{W_{f/h}^{[\Gamma]}(x, b; P_2, S; \mu)} \\ &= \left(\frac{P_1^+}{P_2^+}\right)^{K(b, \mu)} \frac{\mathbb{C}_H(xP_1^+, \mu)}{\mathbb{C}_H(xP_2^+, \mu)} + \mathcal{O}(\lambda^2) \end{aligned}$$

A. Vladimirov and A. Schaefer, PRD 101, 074517]



- Construction of TMDPDF matrix element:

$$W_{f/h}^{[\Gamma]}(b; \ell, L; v, P, S; \mu) = \langle h(P, S) | \bar{q}_f(b + \ell v) \Gamma \mathcal{U}[\mathcal{C}(\ell, v, b, L)] q_f(0) | h(P, S) \rangle$$

3pt of pion on the lattice

- Large separation limit achieved by constant fit: $W^{[\Gamma]} = 2E_P \lim_{0 \ll \tau \ll t} \frac{C_{3pt}(P, \mathcal{C}, t, \tau, \Gamma)}{C_{2pt}(P, t)}$
- Parametrization via (Lorentz) invariant amplitudes: [B. U. Musch, et al, PRD 85, 094510]

$$W^{[\gamma^\mu]}(b; L; v, P, S) = P^\mu \tilde{A}_2 + \frac{M^2}{v \cdot P} v^\mu \tilde{B}_1 - iM\epsilon^{\mu\nu\alpha\beta} P_\nu b_\alpha S_\beta \tilde{A}_{12} - iM^3 \epsilon^{\mu\nu\alpha\beta} b_\nu (Lv_\alpha) S_\beta \tilde{B}_8 - iM^2 b^\mu \tilde{A}_3 + \dots$$

- Combine invariant amplitudes to build twist-2 and twist-3 TMDPDFs:

$$f_1(b^2, P^+) = P^+ (\tilde{A}_2(b^2) + M^2 \frac{v^+}{(v \cdot P) P^+} \tilde{B}_1(b^2)),$$

$$e(b^2, P^+) = P^+ \tilde{A}_1(b^2)$$

f₁ and e for both pion and proton !

Lattice setup

- Calculations on CLS ensemble H101

name	β	$L^3 \times T$	$a[\text{fm}]$	$\kappa_l = \kappa_s$	m_π	m_K	$m_\pi L$	$L[\text{fm}]$	conf
H101	3.4	$32^3 \times 96$	0.0854	0.13675962	422	422	5.8	2.7	2016

Table 1: Parameters of the H101 CLS ensemble used in the present study.

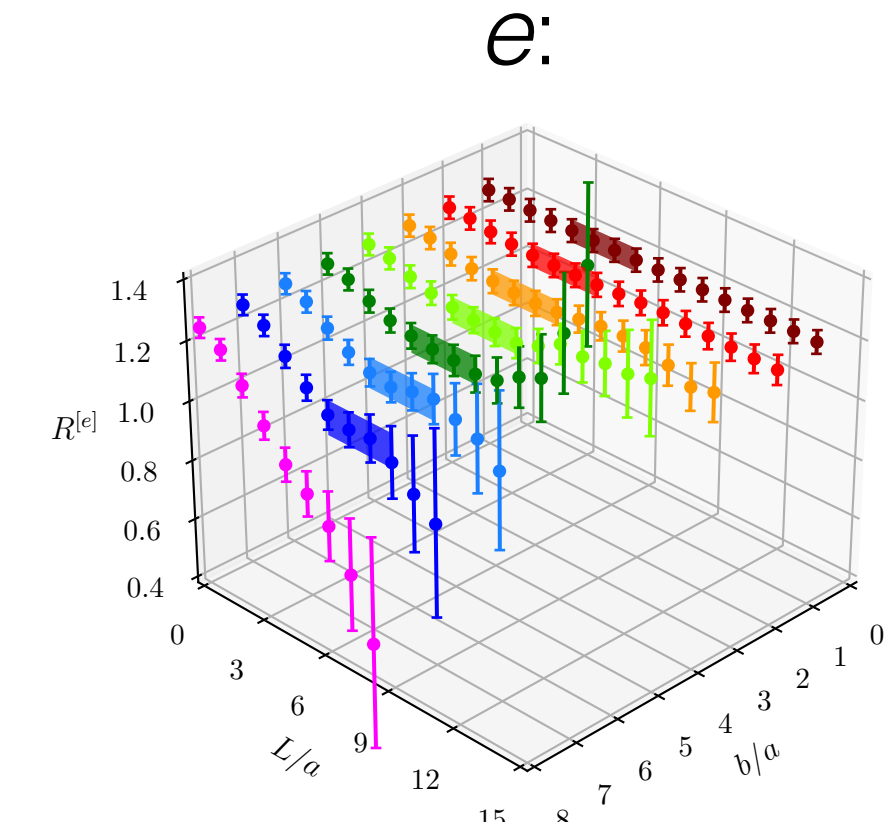
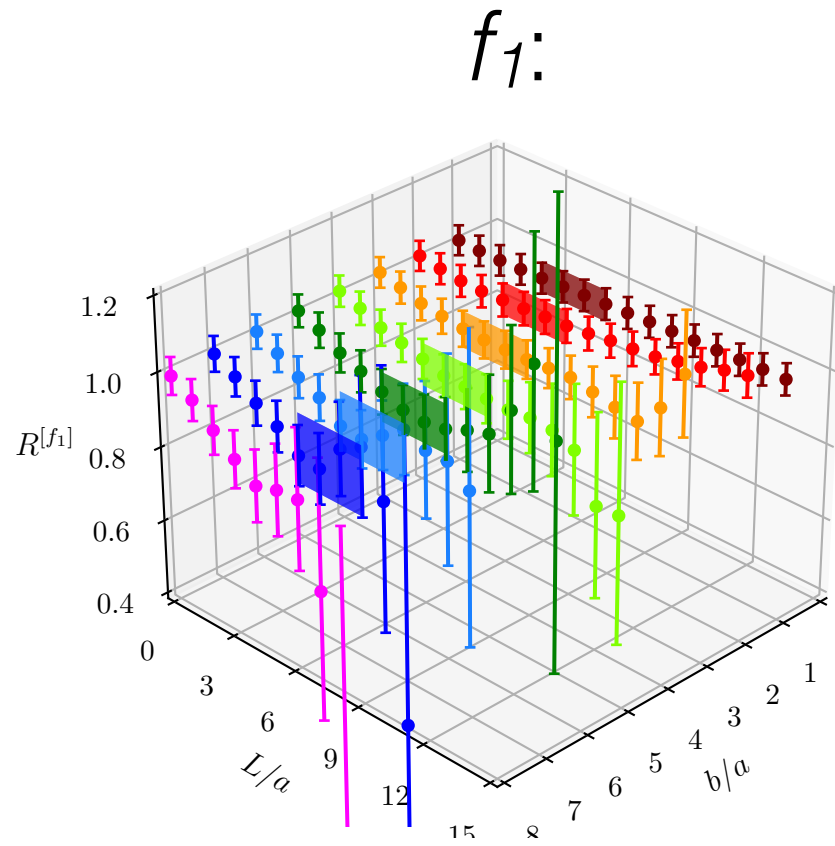
- The hierarchy needs to be respected for the factorization theorem

$$\frac{P^-}{P^+} \ll 1, \frac{1}{|b|P^+} \ll 1, \frac{|b|}{L} \ll 1, \frac{\ell}{L} \ll 1, \ell\Lambda_{\text{QCD}} \ll 1$$

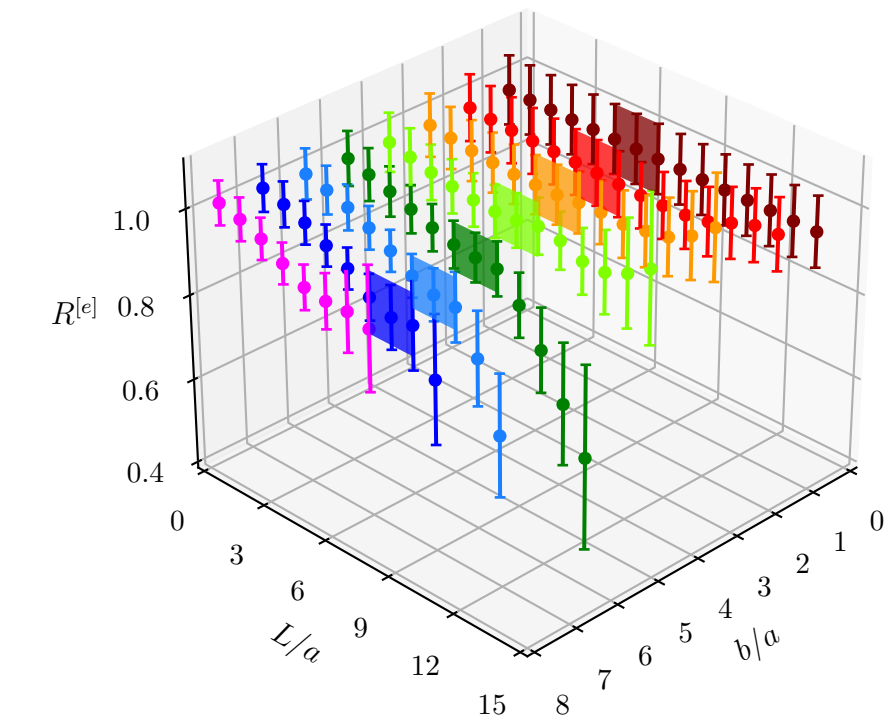
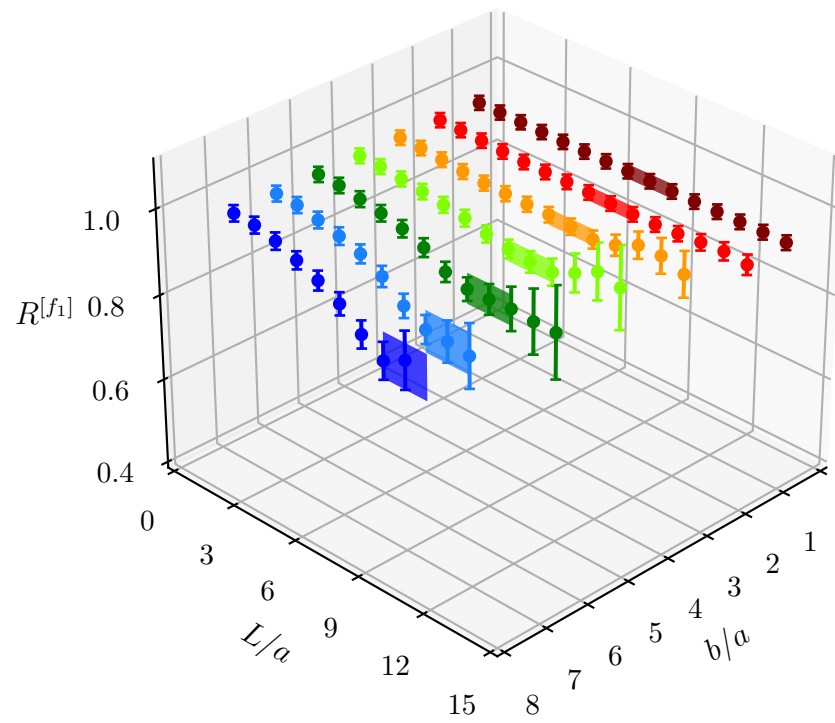
- HYP smearing + Momentum smearing
- Multiple source per configuration
- Momenta: $P^z = \{0, 1, 2, 3, 4, 5\} \times 2\pi/L$
- $|=0, 0 \leq L/a \leq 9 \sim 20, 0 \leq b/a \leq 8, 0 \leq t/a \leq 9/11$

Constant fit for the ratio at $P_1/P_2=3/2$

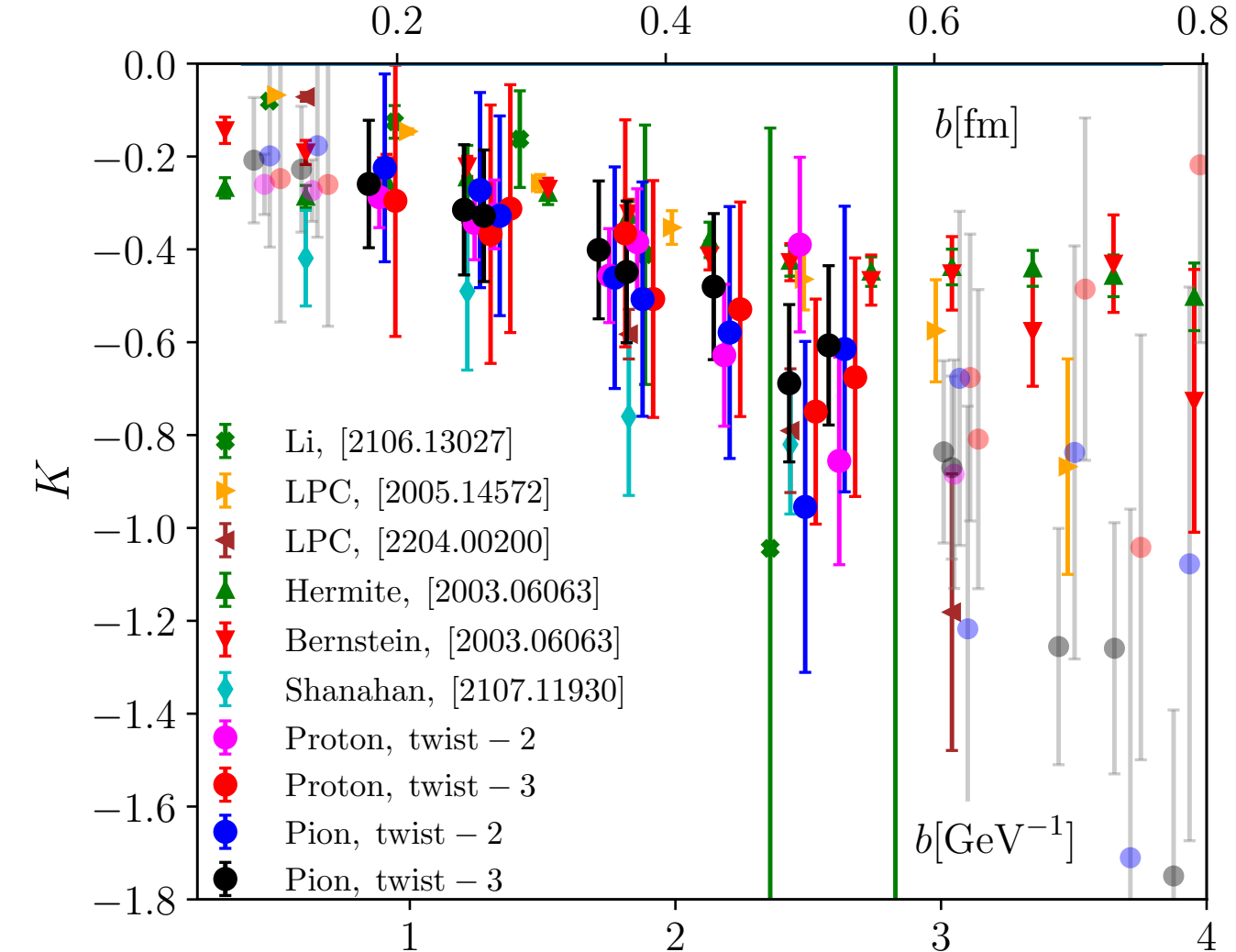
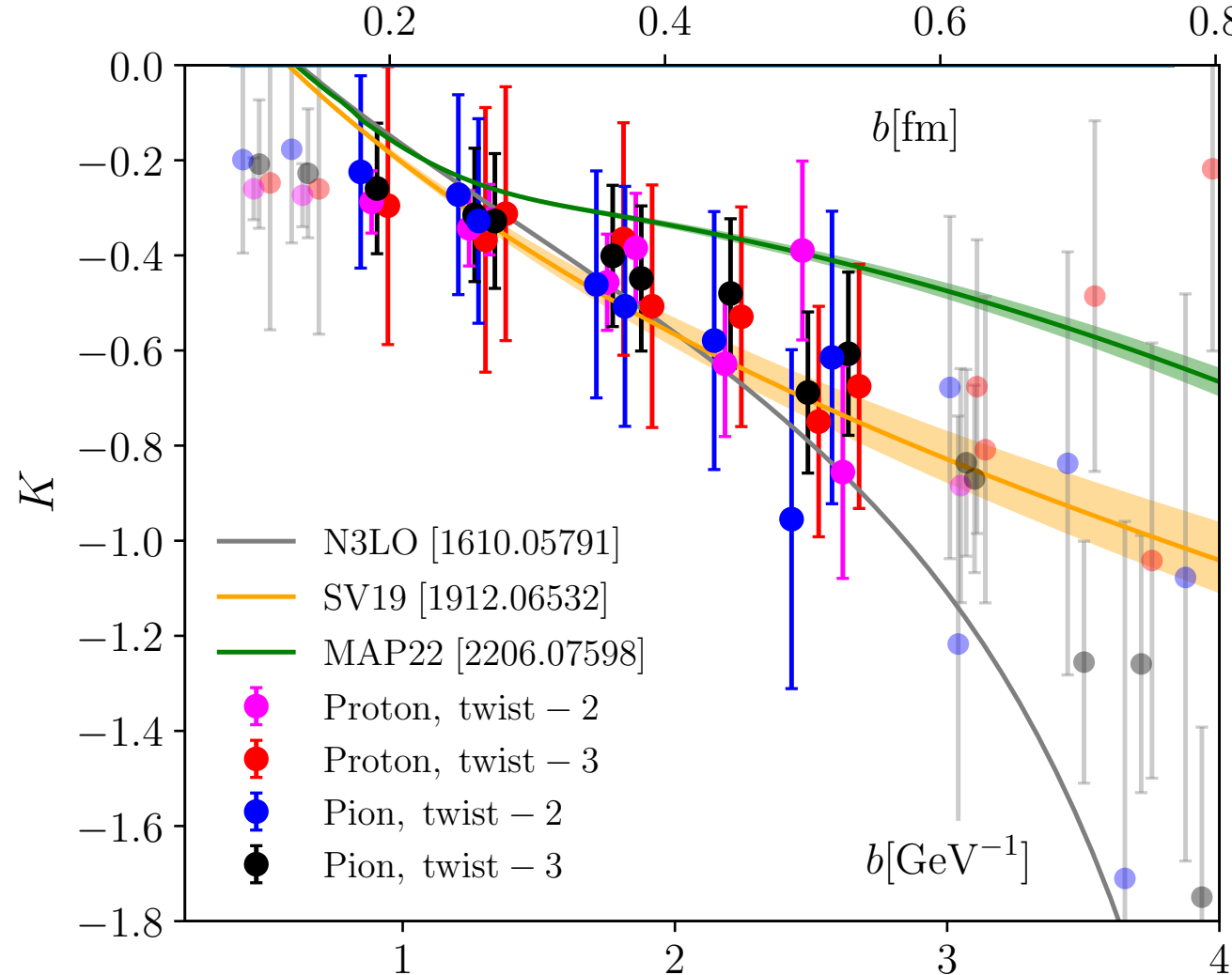
pion:



proton:

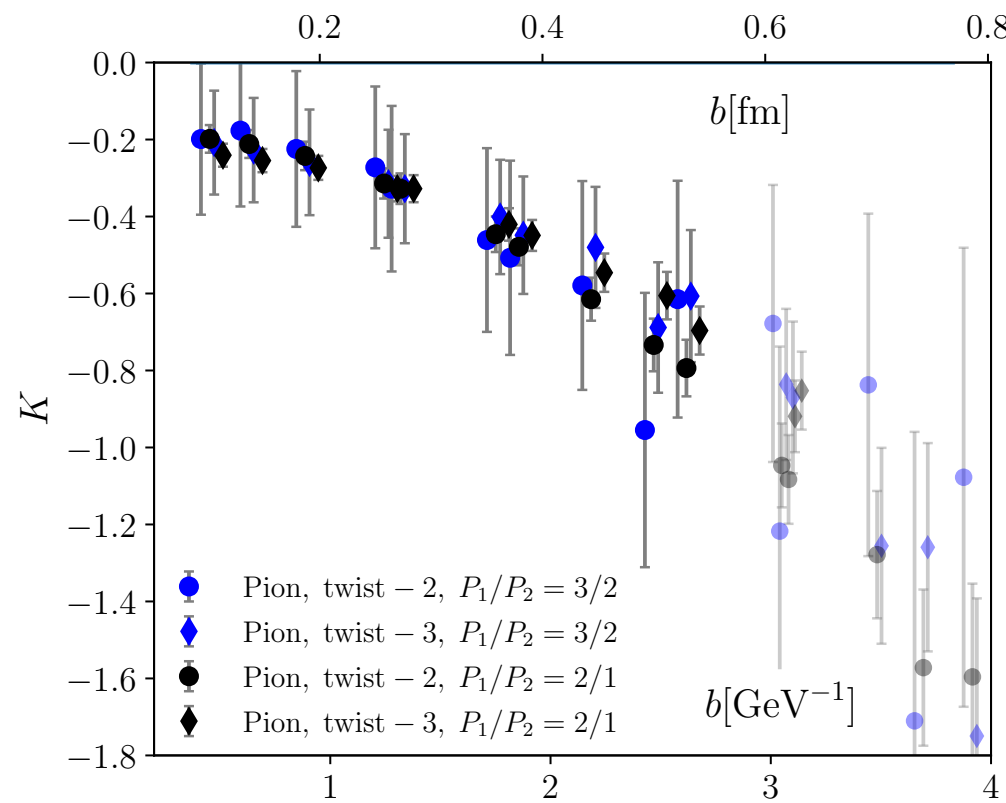
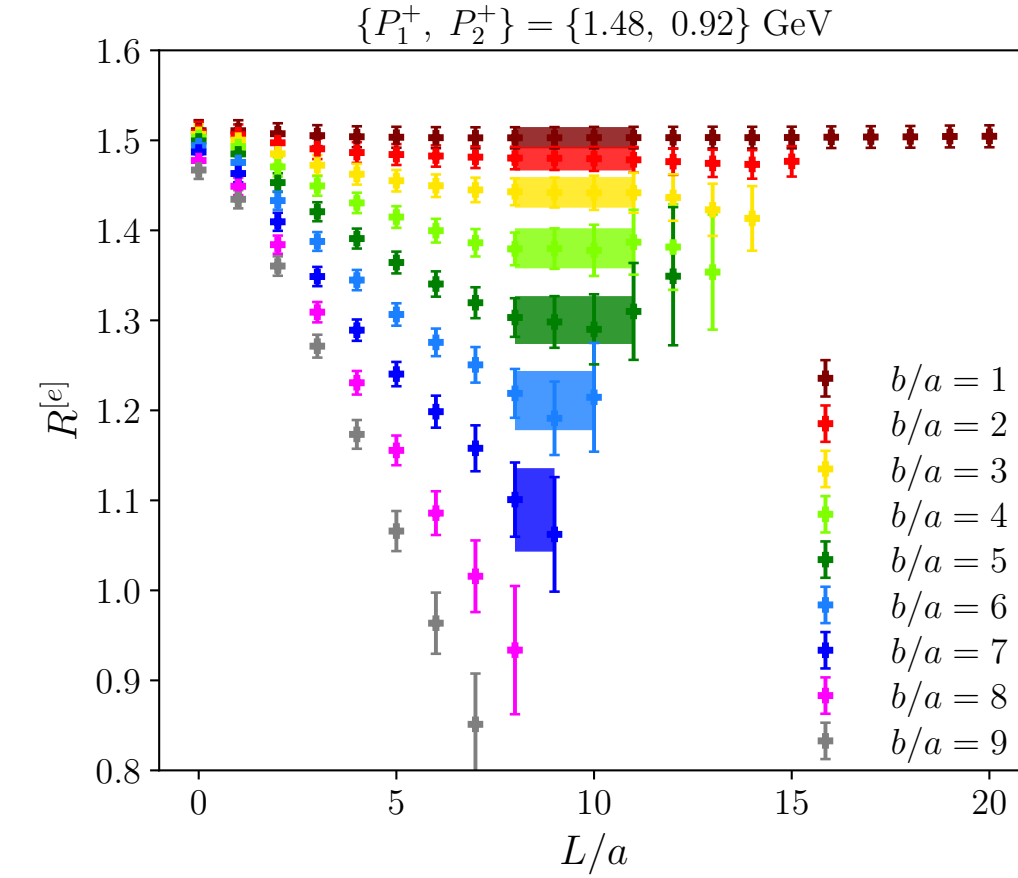
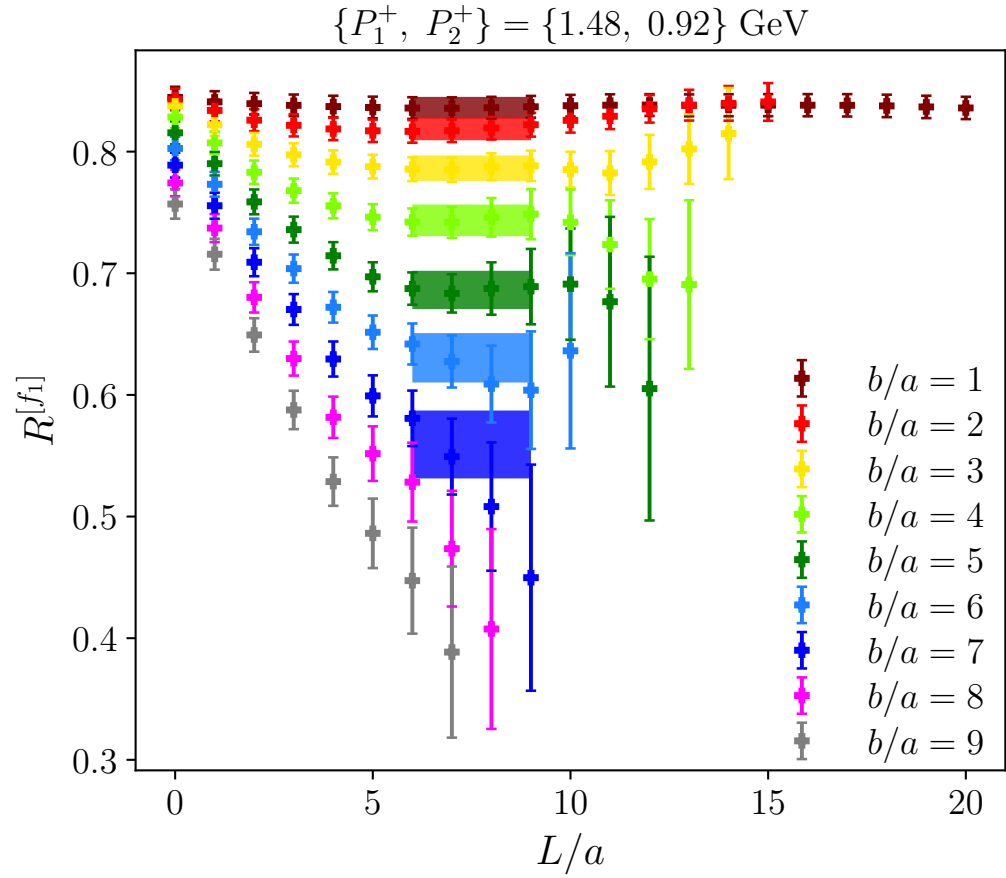


Collins-Soper kernel from $P_1/P_2=3/2$



- Consistent results for pion and proton, twist-2 and twist-3
- This study agrees with SV19 phenomenological calculations and is lower than MAP22
- Lattice computations display qualitatively similar behavior
- The discrepancies can be understood as systematic effects

Collins-Soper kernel from $P_1/P_2=2/1$



- Smaller statistical errors but probably larger systematical errors
- Better identified plateaus
- Very close central values for CS kernel from different momentum pairs (power corrections suppressed)

Summary

- CS kernel calculated using lattice QCD in different ways on two different CLS ensembles
- Good agreement among different lattice extractions
- Universality of the lattice-determined CS kernel was observed
- High-precision determination of CS kernel is in reach